The effect of diffusive solvent relaxation on ultrafast electron transfer within the methyl viologen–hexacyanoferrate complex in trehalose–water glass

ARTICLE *in* CHEMICAL PHYSICS LETTERS · AUGUST 2004

Impact Factor: 1.9 · DOI: 10.1016/j.cplett.2004.06.057

2 AUTHORS, INCLUDING:

Ken Spears
University of Michigan
95 PUBLICATIONS **2,189** CITATIONS

SEE PROFILE

Available online at www.sciencedirect.com
SCIENCE DIRECT®
Chemical Physics Letters 393 (2004) 397–402
CHEMICAL PHYSICS LETTERS
www.elsevier.com/locate/cplett

The effect of diffusive solvent relaxation on ultrafast electron transfer within the methyl viologen-hexacyanoferrate complex in trehalose–water glass

Andrew M. Moran, Kenneth G. Spears *

Chemistry Department, Northwestern University, 2145 Sheridan Road, Evanston, IL 60208-3113, USA

Received 16 April 2004
Available online 6 July 2004

Abstract

Electron transfer rate were measured for methyl viologen-hexacyanoferrate and methyl viologen-hydroquinone complexes in solution and in trehalose–water glass matrices. Rates measured in the glass were a factor of 2.5–3 smaller than those observed in aqueous solution, whereas linear absorption spectra were shifted by less than 300 cm^{-1} with only minor differences in line shape. Our data in the trehalose–water glass are consistent with a predominantly aqueous local environment. Electron transfer rate data are modeled by allowing 10% of the solvent reorganization in the glass to proceed diffusively.

1. Introduction

The semiclassical Marcus/Hush formulation of electron transfer kinetics treats relaxation of the solvent polarization as occurring instantaneously on the time scale of the reaction [1,2]. Solvent reorganization enters the calculation at the level of an equilibrium barrier and reaction trajectories proceed along steepest-descent paths [3]. However, this picture does not hold when relaxation and reaction rates are comparable. Dynamical bath effects cause deviations from the equilibrium trajectory in which the system must traverse a higher potential barrier. The reaction slows down. This issue was treated theoretically by several authors [3–8]. Experimental tests of the theory were complicated by the difficulty of isolating the solvent relaxation in various environments without modifying other important energetic parameters [9–15].

We propose that a comparison of electron transfer rates in aqueous solution and trehalose–water glass constitute a well-defined case in which rate differences are dominated by bath dynamics, and deviations in equilibrium energetic properties are minimal. Two complexes are considered here: the methylviologen-hexacyanoferrate (MVHF) and the methylviologen-hydroquinone (MVHQ) ion-pairs. Structures of the component ions are shown in Fig. 1. The focus of our study is the interpretation of environment-dependent rates, which occur with only minor differences in the linear absorption spectra. We suggest that our data are best interpreted in terms of diffusive solvent reorganization. To our knowledge, this work represents the first report of picosecond electron transfer rates between ion-pairs in a trehalose matrix. The general significance of this work is to develop a more complete understanding dynamic environmental effects on electron transfer rates, since many practical applications of electron transfer, such as novel photovoltaic systems, will involve molecules embedded in a solid state matrix.

The observation of indistinguishable absorption spectra in trehalose–water and aqueous solution is not unique to our complexes. For example, absorption and fluorescence spectra of rhodamine 6G and cytochrome *c* do not change in the trehalose matrix with respect to aqueous solution [16]. It was proposed that an aqueous solvation layer surrounds the chromophores. Recent vibronic side band luminescence measurements of Gd^{3+}

* Corresponding author. Fax: +8474917713.
E-mail address: k-spears@northwestern.edu (K.G. Spears).

0009-2614/$ - see front matter © 2004 Elsevier B.V. All rights reserved.
doi:10.1016/j.cplett.2004.06.057

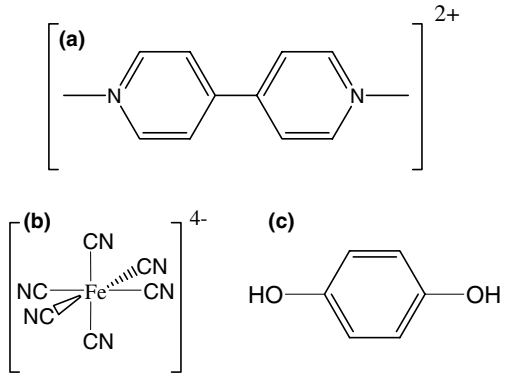

Fig. 1. Ion-pair components: (a) methyl viologen; (b) hexacyanoferrate; (c) hydroquinone.

in a trehalose matrix show that water molecules comprise the first two solvation layers and that the effect of trehalose is to weaken the hydrogen bonds between the first and second solvation layers [17]. Hole-burning experiments for cytochrome *c* in dry trehalose film show significantly more spectral diffusion compared to solution [18]. Single molecule studies also suggest greater heterogeneity [16]. A picture in which interconversion between distinct conformations is inhibited by reduced anharmonic motion in the glass was suggested [19–21]. These data point to a microscopic picture in which both translational and reorientational motion are considerably damped for large molecules like proteins. However, it is not clear that dynamics in smaller molecules are influenced by the same forces. Local effects such as hydrogen bonding may couple more strongly to nuclear motion, making explicit consideration of these coordinates essential for kinetic predictions.

2. Experimental methods

The experimental design is to directly pump the charge transfer absorption at 500 nm and then monitor the decay of the viologen radical cation at 610 nm. The apparatus allowed monitoring the transient absorption over the visible range. Experiments were carried out using an amplified Ti:Sapphire laser system described in prior publications [22]. The output of the compressor is centered at 805 nm with a spectral bandwidth of 22 nm. The 90 fs duration was determined by autocorrelation assuming a hyperbolic secant squared temporal pulse profile. A 500 nm pump beam was generated using a laboratory built near-IR optical parametric amplifier (OPA). The pump beam was centered at 500 nm had a 2 $\mu J\,pulse^{-1}$ with a bandwidth of $\sim$15 nm. Continuum probe pulses were generated by focusing the compressed 800 nm beam into a 3-mm thick piece of optical grade sapphire with a 15 cm focal length lens. Pump and probe beams were focused to spot sizes of 600 and 300 μm, respectively. The beams crossed at an angle of 10°. After the sample, the probe beam was coupled into an Ocean Optics spectrograph using an optical fiber. Transient absorption from 400 to 750 nm over a time range of 0–2 ps was done by alternating pump on/off pulses with electronics and software by Ultrafast Systems.

The chemicals D-(+)-trehalose dihydrate, potassium hexacyanoferrate (II), methyl viologen dichloride, and hydroquinone were purchased from Aldrich and used as received. Ethylene glycol was purchased from Fischer. Solutions of MVHF and MVHQ were prepared using 1:1 ratios of the ion-pair components at optical densities of 0.6–0.9 A/mm. Extinction coefficients and equilibrium constants of MVHF and MVHQ are given in [23] (69 $M^{-1}\,cm^{-1}$) and [24] (115 $M^{-1}\,cm^{-1}$), respectively.

Trehalose–water mixtures were prepared using a 5% w/w aqueous solution. Several drops of the solution were placed on a glass cover slip and allowed to dry at various temperatures. The sample is a glassy state with different thicknesses on the glass cover slip. The data reported here involve samples prepared by drying either 25 or 75 °C. We found that the mass of the sample converged to a lower limit in 24 h. The mass percentage of trehalose was 80% and 95% for the samples dried at 25 and 75 °C, respectively.

3. Theory

Our aim is to describe environmental effects on the electron transfer rate. To that end we focus on relative rates as opposed to calculations of absolute rates. The approach involves a single equilibrated reaction coordinate in lieu of a sum over parallel vibronic channels. This picture is sufficient for ion-pairs undergoing similar structural changes in different solvents.

In the formalism of Mukamel and co-workers [6,7] the rate constant is written

$$K = \frac{2\pi(V^2/\hbar)\sigma(\delta_a - E)}{1 + \sqrt{2\pi}(V^2/\Delta\hbar)[\tau(q_a) + \tau(q_b)]}, \tag{1}$$

where $\sigma(\delta_a - E)$ the linear absorption line shape, E is a free energy gap, V is a matrix coupling element, δ_a is reorganization energy, Δ represents the coupling strength between the solute and bath, and $\tau(q_a)$ is the bath relaxation time for perturbation near $\delta_a - E$. In the static limit, Eq. (1) can be rewritten in activated form

$$K = \frac{\sqrt{2\pi}(V^2/\Delta\hbar)\exp\left(-\Delta G^*_{ab}/k_B T\right)}{1 + \sqrt{2\pi}(V^2/\Delta\hbar)[\tau(q_a) + \tau(q_b)]}, \tag{2}$$

where

$$\Delta G^*_{ab} = \frac{(E - \delta_a)^2}{2|\delta_a - \delta_b|}. \tag{3}$$

In the static limit ($\kappa = 0.1$), the system-bath coupling strength is calculated using the Pade approximant [25]

$$\Delta = \Gamma_{\text{fwhm}} \frac{1 + 0.85\kappa + 0.88\kappa^2}{2.355 + 1.76\kappa}. \tag{4}$$

The strength of this formalism is that the bath relaxation time is defined for arbitrary functional form using a solvation correlation function $M(t)$. The $M(t)$ reported for water in Ref. [26] is used in our calculations. The relaxation time in state a is written as

$$\tau(q_a) \equiv \exp\left(\frac{-q_a^2}{2}\right) \int_0^\infty dt \left\{ \frac{1}{\sqrt{1 - M^2(t)}} \exp\left[\frac{q_a^2 M(t)}{1 + M(t)}\right] - 1 \right\}, \tag{5}$$

where q_a is related to the reaction activation energy by

$$q_a^2 \equiv \frac{(E - \delta_a)^2}{k_B T |\delta_a - \delta_b|}. \tag{6}$$

The numerator of Eq. (1) is simply the golden rule expression for reaction rate. The denominator contains the adiabaticity parameter $\sqrt{2\pi}(V^2/\Delta\hbar)[\tau(q_a) + \tau(q_b)]$, which corrects the golden rule expression for bath dynamics occurring on the time scale of the reaction. We ignore the term $\tau(q_b)$, which represents thermally activated charge transfer from the ground to excited state.

We take a similar approach to Barbara and coworkers [27] for describing relaxation that occurs on the time-scale comparable to the reaction. The classical reorganization energy is partitioned into fast and slow components as

$$\lambda_{\text{Classical}} = \lambda_{\text{Fast}} + \lambda_{\text{Slow}}. \tag{7}$$

The ground and excited state potential energy surfaces are then expressed in terms of fast X_{Fast} and slow X_{Slow} solvation coordinates as

$$F_{\text{gr}}(X_{\text{Fast}}, X_{\text{Slow}}) = \lambda_{\text{Fast}} X_{\text{Fast}}^2 + \lambda_{\text{Slow}} X_{\text{Slow}}^2, \tag{8}$$

$$F_{\text{ex}}(X_{\text{Fast}}, X_{\text{Slow}}) = \lambda_{\text{Fast}}(X_{\text{Fast}} - 1)^2 + \lambda_{\text{Slow}}(X_{\text{Slow}} - 1)^2 - \Delta G^0. \tag{9}$$

The effective free energy gap can then be written as

$$\Delta G^0_{\text{eff}}(X_{\text{Slow}}) = \lambda_{\text{Slow}}(2X_{\text{Slow}} - 1) + \Delta G^0. \tag{10}$$

Equilibration with respect to X_{Fast} is assumed to occur instantaneously, whereas motion with respect to X_{Slow} is described by the diffusion equation

$$\frac{\partial \rho(X_{\text{Slow}}, t)}{\partial t} = D\left(\frac{\partial}{\partial X_{\text{Slow}}} + \frac{1}{k_B T} \frac{\partial F_{\text{ex}}}{\partial X_{\text{Slow}}} \right) \rho(X_{\text{Slow}}, t) - K(X_{\text{Slow}}) \rho(X_{\text{Slow}}, t), \tag{11}$$

where $\rho(X_{\text{Slow}}, t)$ represents population, $k(X_{\text{Slow}})$ is the rate constant, and the diffusion coefficient is defined by

$$D = \frac{k_B T}{2\lambda_{\text{Slow}} \tau_{\text{Slow}}}. \tag{12}$$

The relaxation time of the slow coordinate is τ_{Slow}.

Comparison to experimental measurements are made by calculating the decay of the survival probability using $P(t) = \int_{-\infty}^{\infty} dX_{\text{Slow}} \rho(X_{\text{Slow}}, t)$. The function $P(t)$ is generally not exponential in form. The average time is computed as

$$\tau = \int_0^\infty dt P(t). \tag{13}$$

4. Results

Linear absorption spectra for the MVHF complex in water and ethylene glycol are presented in Fig. 2a. A red shift in the peak position and slight increase in width is seen as the fraction of ethylene glycol is increased. Linear absorption spectra in trehalose are shown in Fig. 2b. The dominant effect is a moderate increase in width as the fraction of water decreases. The peak also shifts to the red slightly.

Linear absorption spectra measured for the MVHQ complex in aqueous solution and in 95% trehalose are shown in Fig. 3. The width of the absorption band increases in trehalose by 16 nm (630 cm^{-1}), but the absorption maximum only shifts by ~10 nm. The increase in width occurs only on the red side of the peak.

Transient absorption data for various samples of MVHF are shown in Fig. 4a–d. The rate increases by a factor of ~2 in ethylene glycol with respect to water (Table 1). The rates measured in trehalose depend on the water content of the glass. The rate decreases by factors of ~1.9 and 2.5 for matrices dried at 25 and 75 °C, respectively. Published studies of glass transition temperatures (T_g) [28] were used to compute the approximate

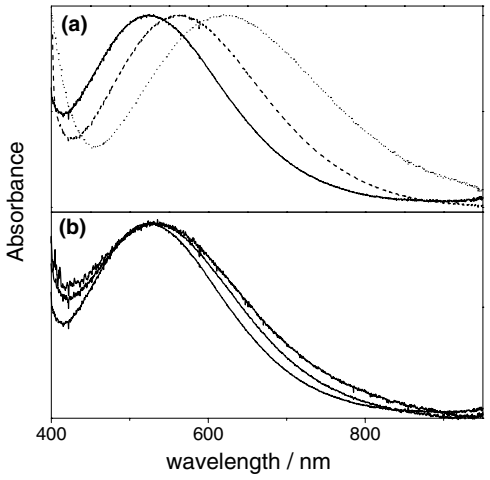

Fig. 2. Absorption spectra for the MVHF complex: (a) in water (solid), a 1:1 mixture of water and ethylene glycol (dash), and pure ethylene glycol (dot); (b) in aqueous solution (narrowest line width), in 80% trehalose-glass, and in 95% trehalose-glass (greatest line width).

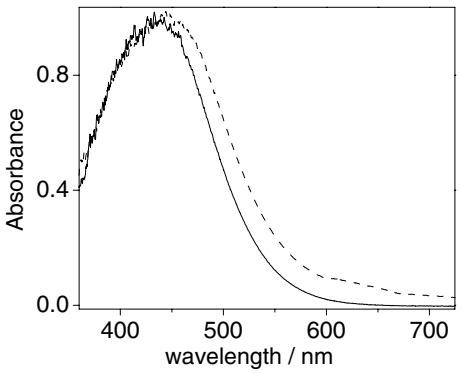

Fig. 3. Absorption spectra of the MVHQ complex in aqueous solution (solid) and in 95% trehalose-glass.

T_g as 47 °C for the 80% sample and +45 °C for the 95% sample. Kinetics measured for the 95% sample both at room temperature and at 50 °C gave indistinguishable rates, which suggests that the rate is not sensitive to the glass transition temperature of the bulk. However, a detailed temperature dependent study will be necessary to reach solid conclusions on this issue.

Transient absorption spectra for the MVHQ complex are shown in Fig. 5. The rate is ~10 times that measured for the MVHF complex. The rate is a factor of ~3 slower in trehalose compared to water.

Table 3 contains calculated time constants (Eq. (13)) incorporating diffusive solvent relaxation. Parameters used in these calculation are given in Table 2 [29]. The diffusive relaxation time τ_{Slow} (15 ps) was substituted for the 0.88 ps exponential argument in $M(t)$. All other parameters in $M(t)$ were fixed to literature values for water [26]. The calculation is relatively insensitive to the choice of the τ_{Slow} when it is longer than the $K(X)^{-}1$; the time constants computed for $\tau_{Slow} = 15$ and 75 ps differ by less than by less 0.3 ps at 10% slow reorganization. The initial population distribution was taken to be a Gaussian function centered at $X = 0.5$ with a standard deviation of 0.11. This distribution is localized within the excited state potential well, but is wide enough to represent a fairly heterogeneous sample. Values in Table 3 should be considered in reference to a time constant of 0.79 ps, which is calculated with 0% slow reorganization and the $M(t)$ for water. This value represents the measurement in aqueous solution.

Table 1
Single exponential time constants measured for the two complexes

Complex	Matrix	Time constant/ps
MVHF	Ethylene glycol	1.5
	Water	3.4
	80% Trehalose	6.5
	95% Trehalose	8.5
MVHQ	Water	0.2
	95% Trehalose	0.6

5. Discussion

In the inverted region of electron transfer, a decrease in rate for constant electronic coupling can be attributed to either an increase in the free energy gap or decrease in reorganization energy. For example, the faster kinetics measured for MVHF in ethylene glycol with respect to

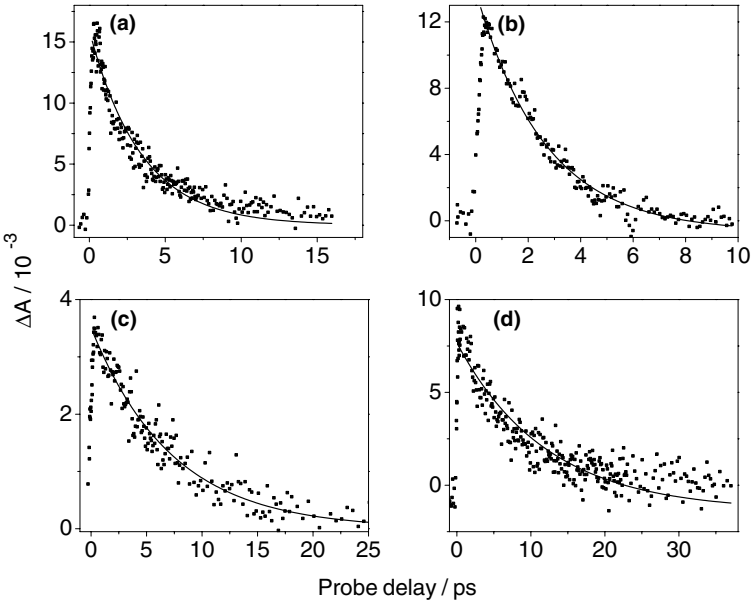

Fig. 4. Transient absorption for MVHF measured at 610 nm in: (a) water; (b) ethylene glycol; (c) 80% trehalose/trehalose–water; (d) 95% trehalose/trehalose–water. The pump wavelength is 500 nm.

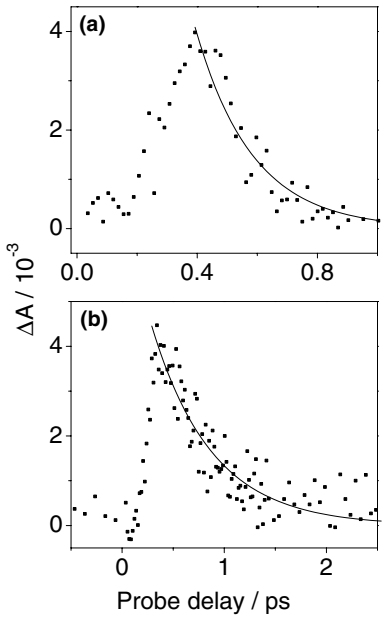

Fig. 5. Transient absorption for MVHQ measured at 610 nm in: (a) water; (b) 80% trehalose/trehalose–water. The pump wavelength is 500 nm.

Table 2
Modelling parameters

ΔG^{0a}	$-9550\ cm^{-1}$
$\lambda_{Classical}{}^{a}$	9303 cm
τ_{Slow}	15 ps
V	$200\ cm^{-1}$
κ^{b}	0.1
$\Gamma_{fwhm}{}^{c}$	$7600\ cm^{-1}$
Δ^{d}	$3285\ cm^{-1}$

[a] Parameters taken from [29].
[b] Represents the static line broadening limit.
[c] FWHM of absorption band Fig. 2a.
[d] Eq. (4).

Table 3
Calculated time constants (Eq. (13))

$\lambda_{Slow}/\lambda_{Classical}$	Time constants/ps
0.00	1.2
0.05	1.6
0.10	2.2
0.15	3.0
0.20	4.0
0.25	4.9
0.30	5.7
0.35	6.6
0.40	7.2

water is interpretable by inspection of the spectral shift in Fig. 2a; The free energy gap is smaller in ethylene glycol ($\varepsilon = 31.7$), and this results in a more rapid electron transfer. The analysis of linear absorption spectra and kinetics in water and trehalose involves the interplay of three parameters: the homogeneous width (Γ_{fwhm}), the inhomogeneous width, and the free energy gap. The homogeneous and inhomogeneous widths combine to give the total line width, while the sum of the free energy gap and classical reorganization energy (determined by the homogeneous width) gives the position of the absorption band. The minor spectral differences in Fig. 2b indicate that any change in free energy must be compensated for by the reorganization energy in order for the absorption band to reside at the same wavelength in aqueous solution and in the trehalose-glass.

Rationalization of our solvent-dependent rates in the context of classical transition state theory requires a concomitant increase in the free energy gap and decrease in the classical reorganization energy. However, the free energy gap should not increase in a medium with a smaller dielectric constant without a significant geometry change within the complex. The interionic distance in an ion pair system might change the energy gap, but a soft matrix is unlikely to greatly perturb this coordinate. Dielectric relaxation measurements [30,31] of trehalose–water mixtures show a continuous decrease in the static dielectric constant with increasing trehalose content ($\epsilon = 62$ at 55% w/w trehalose–water), [30] although matrices with 5–20% water were not reported. As suggested in the Section 1, the innermost solvation layers are likely to be mostly composed of water. The relevant dielectric properties are therefore not obtained from bulk measurements. In addition, resonance Raman spectra shows that ground state frequencies for modes coupled to the electron transfer and their relative intensities are indistinguishable between solution and trehalose, which suggests that internal geometries of the complex in the two environments are similar [32].

We model the electron transfer rates in the glass by using a solvent coordinate similar to pure water X_{Fast} and a second coordinate that relaxes slowly on the timescale of the reaction X_{Slow}. Our calculations (Table 3) shows that an increase in the decay time constant for MVHF in trehalose is consistent with ~10% fraction of slow reorganization (The rate slows down by a factor of 2.5–3.). The analysis suggests that a small amount of a diffusive solvent relaxation can affect electron transfer rates in a manner that can not be directly predicted given linear absorption spectra. The identity of this new coordinate is undefined in our model. However, a reasonable picture can be proposed.

Pure aqueous relaxation is dominated by dipole reorientation, so it is likely that hindered rotational motion is primarily responsible for a slower relaxation time. We take this general idea to be robust, and acknowledge that discussion involving a more well-defined microscopic model is speculative. The next level of interpretation should point to specific independent or cooperative motion within the solvation layers. We base a likely microscopic picture on the following two premises: (i) The first and second solvation layer of the

ion-pair in the glass is predominantly water. Linear absorption measurements support this premise. (ii) Hydrogen-bonding between the first and second solvation layers is different in the glass than in solution. This premise is consistent with a recent study involving the Gd^{3+} ion [17], which revealed a weaker interaction between the first and second layers in a trehalose matrix compared to free solution. These premises lead to the picture in which diffusive reorganization is associated with damping of rotational motion outside the first solvation layer. The hydrogen bonding network between outer solvation layers and the trehalose matrix is thought to become increasingly rigid as the distance from the ion-pair increases. Future investigations will monitor the temperature effects on electron transfer rate over a wide range of temperatures in order to examine the unique changes in the solvation dynamics that might be occurring in this system.

Acknowledgements

We thank the US Department of Energy, Office of Science (Grant DE-FG02-91ER14228), for financial support.

References

[1] M. Bixon, J. Jortner, in: S.A. Rice (Ed.), Advances in Chemical Physics, Wiley, New York, 1999.
[2] R.A. Marcus, J. Chem. Phys. 24 (1956) 966.
[3] B.M. Hoffman, M.A. Ratner, Inorg. Chim. Acta 243 (1996) 233.
[4] G.E. McManis, M.J. Weaver, J. Chem. Phys. 90 (1989) 912.
[5] J.T. Hynes, J. Phys. Chem. 90 (1986) 3701.
[6] M. Sparpaglione, S. Mukamel, J. Chem. Phys. 88 (1988) 4300.
[7] M. Sparpaglione, S. Mukamel, J. Chem. Phys. 88 (1988) 3263.
[8] H. Sumi, R.A. Marcus, J. Chem. Phys. 84 (1986) 4894.
[9] E. Akesson, A.E. Johnson, N.E. Levinger, G.C. Walker, T.P. DeBruil, P.F. Barbara, J. Chem. Phys. 96 (1992) 7859.
[10] T. Haberle, J. Hirsch, F. Pollinger, H. Heitele, M.E. Michel-Beyerle, H.A. Staab, J. Phys. Chem. 100 (1996) 18269.
[11] T. Kobayashi, Y. Takagi, H. Kandori, K. Kemnitz, K. Yoshihara, Chem. Phys. Lett. 180 (1991) 416.
[12] H. Pal, Y. Nagasawa, K. Tominaga, K. Yoshihara, J. Phys. Chem. 113 (1991) 11964.
[13] L.A. Dick, I. Malfant, D. Kuila, S. Nebolsky, J.M. Nocek, B.M. Hoffman, M.A. Ratner, J. Am. Chem. Soc. 120 (1998) 11401.
[14] L.E. Sinks, M.R. Wasielewski, J. Phys. Chem. A 107 (2003) 611.
[15] G.P. Wiederrecht, W.A. Svec, M.R. Wasielewski, J. Phys. Chem. B 103 (1999) 1386.
[16] E. Mei, J. Tang, J.M. Vanderkooi, R.M. Hochstrasser, J. Am. Chem. Soc. 125 (2002) 2730.
[17] M.S. Navati, A. Ray, J. Shamir, J.M. Friedman, J. Phys. Chem. B 108 (2004) 1321.
[18] V.V. Ponkratov, J. Friedrich, J.M. Vanderkooi, J. Chem. Phys. 117 (2002) 4594.
[19] K.D. Rector, J. Jiang, M.A. Berg, M.D. Fayer, J. Phys. Chem. B 105 (2001) 1081.
[20] F. Librizzi, C. Viappiani, S. Abbruzzetti, L. Cordone, J. Chem. Phys. 116 (2002) 1193.
[21] G. Cottone, L. Cordone, G. Cicotti, Biophys. J. 180 (2001) 931.
[22] T.W. Marin, B.J. Homoelle, K.G. Spears, J.T. Hupp, L.O. Spreer, J. Phys. Chem. A (2002) 1131.
[23] P.M.S. Monk, N.M. Hodgkinson, Electrochim. Acta 43 (1998) 245.
[24] B.G. White, Trans. Faraday Soc. 65 (1969) 200.
[25] S. Mukamel, Principles of Nonlinear Optical Spectroscopy, Oxford University Press, 1995.
[26] R. Jiminez, G.R. Fleming, P.V. Kumar, M. Marconelli, Nature 369 (1994) 471.
[27] K. Tominaga, D.A.V. Kliner, A.E. Johnson, N.E. Levinger, P.F. Barbara, J. Chem. Phys. 98 (1993) 1228.
[28] L.M. Crowe, D.S. Reid, J.H. Crowe, Biophys. J. 71 (1996) 2087.
[29] J.C. Curtis, B.P. Sullivan, T.J. Meyer, Inorg. Chem. 19 (1980) 3833.
[30] S. Mashimo, N. Miura, J. Chem. Phys. 99 (1993) 9874.
[31] T. Matsuoka, T. Okada, K. Murai, S. Koda, H. Nomura, J. Mol. Liq. 98–99 (2002) 317.
[32] Unpublished data.